ChemComm

COMMUNICATION

View Article Online
View Journal | View Issue



Cite this: *Chem. Commun.*, 2019, 55, 4331

Received 6th February 2019,
Accepted 13th March 2019

DOI: 10.1039/c9cc01088b

rsc.li/chemcomm



# A two-target responsive reversible ratiometric pH nanoprobe: a white light emitting quantum dot complex†

Sabyasachi Pramanik, *[ab] Shilaj Roy, [ac] Arup Mondal[c] and Satyapriya Bhandari *[ad]

**Herein we report the use of a white light emitting quantum dot complex (comprising an orange emitting $Mn^{2+}$-doped ZnS quantum dot and greenish-blue emitting zinc-quinolate complex) as a two-target responsive ratiometric reversible pH nanosensor in the physiological range of 6.5–10.3, following changes in their luminescence intensity ratio, color and chromaticity.**

The ability of self-calibration of signal correction, accurate and reliable quantification of a ratiometric optical nanoprobe, compared to an absolute/single intensity dependent nanoprobe, makes them an apt choice for efficiently monitoring physiological or pathological processes, rapid and sensitive treatment of diseases and thus towards advancement of practical clinical diagnosis.[1–10] Usually, the real life application of single-wavelength intensity dependent nanoprobes is limited due to their drawbacks related to intensity fluctuations in the detector, light source, local probe concentration and optical path length.[1–10] While the presence of one signal as a reference of another signal gives an advantage to ratiometric nanoprobes for overcoming the issues related to single-wavelength intensity dependent nanoprobes.[1–10] Thus, there is always a need to develop ratiometric optical nanoprobes, based on the chemical interaction of different emitting species, for their beneficial advantage towards efficient detection of analytes.

On the other hand, the precise measurement of pH is crucial for the purpose of biomedical research (especially, cellular uptake in drug delivery and studying cellular metabolism for diagnosis of various diseases including Alzheimer's disease and cancer) and industrial applications.[1–15] In this regard, several optical nanoprobes and/or methods have been reported for the sensing of pH either in intracellular or extracellular conditions.[1–10] To date, various quantum dot (QD) based single intensity dependent nanoprobes have demonstrated their use as pH indicators and other non-fluorescence based techniques (such as potentiometric measurements) have also demonstrated their use for the detection of pH.[1–10] However, the aforementioned drawbacks of single intensity dependent nanoprobes and uneconomical and inaccurate procedures have limited their use for pH sensing. Instead, ratiometric optical pH sensors, based on the pairs of two different QDs or QD conjugated with dyes/proteins or different polymer materials, have been reported by several research groups.[1–10] However, drawbacks associated with multicomponent QD based optical sensors such as self-absorption, non-radiative energy transfer affected the accuracy of pH detection.[1–10] This creates an opportunity for the fabrication of low-cost, nontoxic single ratiometric optical nanoprobe, towards sensitive detection of pH, followed by overcoming the existing aforesaid issues of multicomponent nanosensors. At present, there are very few reports on the fabrication of single component QD based ratiometric optical pH sensors, having the capability of increasing one signal accompanied by decreasing another signal in the presence of an analyte (also known as two-target responsive systems).[10] For example, dual emitting D-penicillamine decorated $Mn^{2+}$ doped CdSSe/ZnS QD have demonstrated their use for pH sensing, in the range of 4.5–8.5, based on the variation of their luminescence intensity ratio of $I_{510}/I_{610}$.[10] However, the concern of the toxicity of Cd has limited their application potential with regard to maintaining the sustainability of the environment. Thus, it would be noteworthy to construct a low-cost, nontoxic, ratiometric two target responsive nanoprobe (avoiding the use of any heavy metal) for the sensing of pH covering a broad physiological range.

Herein, we report the fabrication of a nontoxic two-target based ratiometric single component white light emitting pH nanoprobe-based on the formation of a greenish blue emitting zinc quinolate complex (with $\lambda_{em}$ = 483 nm) on the surface of an orange emitting $Mn^{2+}$ doped ZnS QDs (with $\lambda_{em}$ = 600 nm). The white light emitting complexed QD is termed herein as the

[a] *Centre for Nanotechnology, Indian Institute of Technology Guwahati, Guwahati-781039, India*
[b] *Department of Chemistry, National Institute of Technology Sikkim, Sikkim-737139, India. E-mail: sabyasachi@nitsikkim.ac.in*
[c] *Department of Chemistry, Indian Institute of Technology Guwahati, Guwahati-781039, India*
[d] *Centre for Nano and Material Sciences, Jain University, Bangalore 562112, India. E-mail: b.satyapriya@jainuniversity.ac.in*

† Electronic supplementary information (ESI) available: Experimental section, Fig. S1–S8 and Tables S1–S5. See DOI: 10.1039/c9cc01088b

white light emitting quantum dot complex (WLE QDC), which is fabricated from a complexation reaction between ligand free $Mn^{2+}$ doped ZnS QD and 5-sulphonic-8-hydroxyquinoline (HQS) ligand. The details of the synthesis of the WLE QDC is described in the ESI.† Importantly, the as fabricated photostable QDC exhibited pure white light, with an intensity ratio ($I_{600}/I_{483}$) of 0.98 and chromaticity of (0.33, 0.34) at pH 6.5. Upon increasing the pH to 10.3, the WLE QDC became orange in color, with an intensity ratio ($I_{600}/I_{483}$) of 10.64 and chromaticity of (0.54, 0.40) while changing the pH from 10.3 to the original pH (6.5) of the WLE QDC restored its pristine luminescence intensity ratio of ($I_{600}/I_{483}$), chromaticity and white color. Notably, the reversibility of the luminescence intensity ratio of ($I_{600}/I_{483}$), chromaticity and color of the WLE QDC depending on the alteration of pH in between 6.5 to 10.3, was found to be effective for four cycles.

The transmission electron microscopic (TEM) analysis showed the average particle size of the $Mn^{2+}$ doped ZnS QDs is 3.2 ± 0.3 nm while the presence of the lattice fringe of 0.3 nm (which is due to the (111) plane cubic ZnS)[11,12] in the high resolution TEM as well as the presence of the characteristics peaks at 28.3°, 47.4°, and 56.4° (which are due to the (111), (220) and (311) lattice planes of cubic ZnS)[11,12] in the powder X-ray diffraction pattern confirmed the formation of orange emitting $Mn^{2+}$ doped ZnS QDs (pH 6.5), with emission maxima at 600 nm and an absorption edge at 320 nm (Fig. S1, S2, ESI† and Fig. 1A, B). Upon complexation with HQS, the luminescence color of the $Mn^{2+}$ doped ZnS QDs (pH 6.6) changes from orange to white (digitally captured with 330 nm light from a spectrofluorimeter) and thus indicating the formation of WLE QDC (pH 6.5; Fig. 1A). The WLE QDC exhibited two emission maxima (Fig. 1B; at an excitation wavelength of 330 nm): one at 600 nm and the other at 483 nm. It is to be noted here that the emission at 600 nm is due to the optical emission feature of $Mn^{2+}$ ions of the $Mn^{2+}$-doped ZnS QD – originated from the recombination of the photoexcited exciton of the ZnS host crystals through lower lying states ($^4T_1$–$^6A_1$) of the $Mn^{2+}$ dopant ions-which is relatively independent of the QD size.[11–14] While the observed emission at 483 nm is solely due to the highest occupied molecular orbital (HOMO)–lowest unoccupied molecular orbital (LUMO) electronic transition of the formed zinc quinolate ($Zn(QS)_2$) complex present on the surface of $Mn^{2+}$ doped ZnS QDs, as per earlier reports.[11,12,15–17] Notably, the $Zn(QS)_2$ complex acted as a quencher of the dopant emission of the $Mn^{2+}$ doped ZnS QDs, which is in accordance with earlier reports.[11,12] While the presence of a new absorption edge at 365 nm – in addition to the absorption edge at 320 nm of $Mn^{2+}$ doped ZnS QDs – also supported the formation of the $Zn(QS)_2$ complex as well as the QDC (Fig. S2, ESI†).[11,12] Interestingly, the changes in the color chromaticity from (0.51, 0.38) to (0.33, 0.34) also supported the formation of WLE QDC from orange emitting $Mn^{2+}$ doped ZnS QDs (Fig. 1C and Table S1, ESI†). It is to be mentioned here that the optimum concentration of HQS was found to be 11.5 μM for the fabrication of WLE QDC (pH 6.5) from 3.0 mL of an aqueous dispersion of $Mn^{2+}$ doped ZnS QDs, having an absorbance of 0.09 at 320 nm (Fig. S3 and Table S1, ESI†). This was calculated followed by monitoring the chromaticity color coordinates approaching towards near white light's chromaticity of (0.33, 0.33)[11,12] with respect to the emission spectrum of QDC at $\lambda_{ex}$ = 330 nm. Notably, the attachment of surface dangling sulphide bonds may be the responsible factor for the attachment of the $Zn(QS)_2$ complex and providing stability to the QDC, as evidently supported from earlier reports.[11,12] As is clear from Fig. 1A, the QDC exhibited white light, with an intensity ratio ($I_{600}/I_{483}$) of 0.98 and chromaticity of (0.33, 0.34), at pH 6.5. Notably, there is

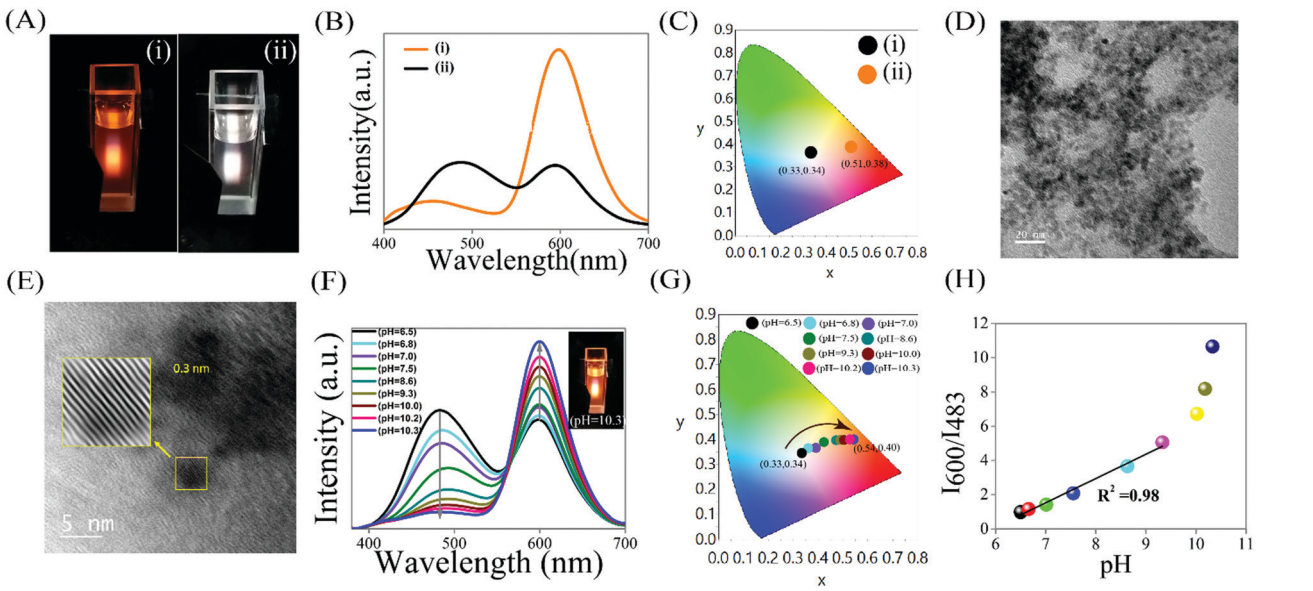


Fig. 1 (A) Digital photographs (B) emission spectra ($\lambda_{ex}$ = 330 nm) and (C) chromaticity color coordinates in CIE diagram of (i) $Mn^{2+}$ doped ZnS QDs (pH 6.6) and (ii) WLE QDC (pH 6.5). (D) Transmission electron microscopy (TEM) image (scale bar = 20 nm), (E) high resolution TEM image (scale bar = 5 nm) and corresponding inverse fast Fourier transformed image (inset) of WLE QDC, (F) Emission spectra ($\lambda_{ex}$ = 330 nm) and (G) chromaticity color coordinates in CIE diagram of WLE QDC upon increasing their pH from 6.5 to pH 10.3. (H) Effect of pH (in the physiological range of 6.5–10.3) on the luminescence intensity ratio ($I_{600}/I_{483}$) of WLE QDC.

 

no significant change in the size and lattice fringes of the QD following complexation with HQS (Fig. 1D and E). This clearly indicated a morphological preservation of QD in WLE QDC. Thus, the presented results clearly indicated the formation of single component WLE QDC.

Now, upon increasing the pH (following base (0.1 M NaOH) treatment), the intensity ratio ($I_{600}/I_{483}$) of WLE QDC gradually increases. For example, when the pH of WLE QDC changes from 6.5 to 10.3, the intensity ratio of $I_{600}/I_{483}$ changes from 0.98 to 10.64 – in addition to the changes in the luminescence color from white to orange and chromaticity from (0.33, 0.34) to (0.54, 0.40) (Fig. 1F and G and Table S2, ESI†). This clearly indicated the changes of luminescence intensity, color and chromaticity of WLE QDC followed by varying their pH. It is to be mentioned here that as the pH of the aqueous dispersion of WLE QDC increased, the intensity of the peak at 483 nm due to the surface $Zn(QS)_2$ complex decreases while the intensity of the peak at 600 nm due to $Mn^{2+}$ dopant of QD increases and as a result of that the overall intensity ratio $I_{600}/I_{483}$ increased. On the other hand, similar observations were made in terms of emission intensity when the pH of individual emitting species (*i.e.* $Mn^{2+}$ doped ZnS QDs and $Zn(QS)_2$ complex attached undoped ZnS QDs) was increased (Fig. S4, ESI†). More specifically, as the pH increased only $Mn^{2+}$ doped ZnS QDs (pH – 6.6) showed an increase in the emission intensity at 600 nm, while a decrease in the emission intensity at 483 nm of $Zn(QS)_2$ complex attached undoped ZnS QDs (pH 6.5) was observed (Fig. S4, ESI†). However, there is no change in the luminescence color and chromaticity of the individual emitting species upon increasing their pH (Fig. S4, ESI†). Fig. 1H clearly shows a variation in the luminescence intensity ratio $I_{600}/I_{483}$ of WLE QDC with respect to pH. Notably, the luminescence intensity ratio $I_{600}/I_{483}$ of WLE QDC increases linearly as the pH of their aqueous solution sequentially changes from 6.5 to 9.3 and on further increasing the pH in the range of 10.0 to 10.3, the increment in the luminescence intensity ratio $I_{600}/I_{483}$ of WLE QDC is much steeper compared to the initial changes. Importantly, the change in the Hue parameter/histogram of the WLE QDC following the changes in the pH from 6.5 to 10.3 further support the convenient quantitative detection of pH (Fig. S5, ESI†). This was calculated using image-J software and following the earlier reports.[18–20] This clearly indicates their excellent sensing ability towards pH in the range of 6.5–10.3.

Interestingly, the observed reversibility in the two emission signals (which is the key factor for the practical utilization of any optical pH nanoprobe)[1–10] and corresponding chromaticity of the WLE QDC, followed by changing the pH from neutral (6.5) to basic (10.3) to again neutral (6.5) for up to four cycles (using the treatment of base followed by an acid; Fig. 2C) clearly indicated their reliability as well as future application potential as an optical nanoprobe for pH sensing. Briefly, upon changing the pH from 6.5 to 10.3, the luminescence color and chromaticity of WLE QDC shifted from white (0.33, 0.34) to orange (0.54, 0.40) and upon further restoring the pH from 10.3 to 6.5 (original pH of WLE QDC), the luminescence color changes from orange to white – in addition to the changes in the chromaticity from (0.54, 0.40) to (0.33, 0.34) (Fig. 2A and B). This clearly endows the reversible nature

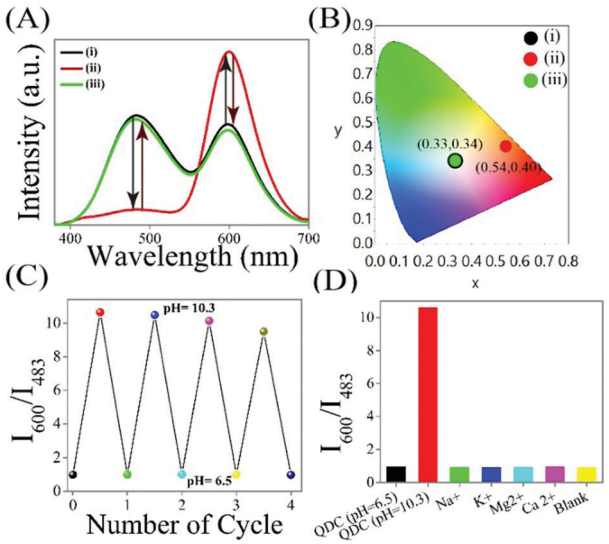


Fig. 2 (A) Reversibility of the luminescence intensity ($\lambda_{ex}$ = 330 nm) and (B) chromaticity color coordinates in the CIE diagram of WLE QDC (pH 6.5) followed by changing the pH to basic (pH 10.3) and then restoring back to the original pH 6.5. (C) 4-Cycle reversibility of luminescence intensity ratio ($I_{600}/I_{483}$) of WLE QDC as pH changed from 6.5 to 10.3 and then 10.3 to 6.5. (D) Comparison of the luminescence intensity ratio (%) of WLE QDC (pH 6.5) followed by addition of $Na^+$ (3.33 μM, pH 6.5), $K^+$ (3.33 μM, pH 6.5), $Mg^{2+}$ (3.33 μM, pH 6.5), $Ca^{2+}$ (3.33 μM, pH 6.5) ions, and solvent (water).

of WLE QDC as a pH nanoprobe. Importantly, the luminescence intensity ratio $I_{600}/I_{483}$ of WLE QDC is reversible when the pH changed from 6.5 to 10.3 for four cycles (Fig. 2C). While there is no significant change observed in the absorption edge of WLE QDC during the reversible pH effect (Fig. S6, ESI†). Additionally, no noticeable change in the luminescence intensity ratio $I_{600}/I_{483}$ of WLE QDC, following addition of interfering substances, was observed (Fig. 2D). Interestingly, in addition, WLE QDC was found to be stable, with respect to their luminescence intensity for 48 hours (at $\lambda_{ex}$ = 330 nm; Fig. S7, ESI†). Furthermore, the WLE QDC was found to be photostable against the continuous irradiation of 330 nm light for half an hour (monitored with respect to their two emission maxima (Fig. S8, ESI†)). The WLE QDC showed a quantum yield (QY) of 4.4% while 4.7% QY was observed for only $Mn^{2+}$ doped ZnS QDs (using quinine sulphate as standard; Table S3, ESI†). It is to be mentioned here that the $Zn(QS)_2$ complex present in the WLE QDC (followed by deconvoluting their emission spectra) showed a QY of 2.3% – which is higher than that of the only zinc quinolate complex (QY = 0.9%) as reported from earlier observations.[21]

As the pH of the WLE QDC increases, the negative charge on the surface of QDC increases, which is confirmed through zeta potential measurements. The as such WLE QDC exhibited a zeta potential value of +19.6 mV at pH 6.5 while a −36.6 mV zeta potential was noted when the pH of WLE QDC increased to 10.3 (Table S4, ESI†). This may be due to the presence of the extra negative charges (in terms of hydroxyl groups) on the surface of WLE QDC at pH 10.3. Additionally, there is no significant change in the zeta potential of the WLE QDC – following the separate addition of different metal ions (such as $Na^+$, $K^+$, $Mg^{2+}$, $Ca^{2+}$) – which ruled

out the possibility of changes in the dipole of the WLE QDC in the presence of the above mentioned interfering metal ions in water (Table S3, ESI†). The pH dependent changes in the luminescence intensity ratio ($I_{600}/I_{483}$), color and chromaticity of WLE QDC is explained based on the combined effect of their two emitting species ($Mn^{2+}$ doped ZnS QD and surface $Zn(QS)_2$ complex). At higher pH such as 10.3, WLE QDC has two consequences: (i) increased negative charges (due to hydroxyl/metal hydroxide passivation) on the surface of $Mn^{2+}$ doped ZnS QD (also supported from the zeta potential measurements) as well as more favourable and feasible binding of acetate (which may be acting as a stabilizer in the present case of the so called ligand free $Mn^{2+}$ doped ZnS QD) leading to enhancement in the luminescence intensity at 600 nm (followed by reducing nonradiative transitions)[22–25] and (ii) the deviation from optimum pH ($\sim$6) of $Zn(QS)_2$ complex (at which their luminescence intensity reached a maximum)[26] as well as the deprotonation of sulphonic acid group leading to the decrease in the luminescence intensity at 483 nm and thus leading to the overall enhancement in the luminescence intensity ratio ($I_{600}/I_{483}$) of WLE QDC. Further changes in the pH from 10.3 to 6.5, returning back to the original luminescence intensity ratio ($I_{600}/I_{483}$), color and chromaticity of WLE QDC is explained based on the higher probability of the non-radiative transition of $Mn^{2+}$ doped ZnS QD leading to a decreased luminescence intensity at 600 nm and approaching towards optimum pH ($\sim$6) of surface $Zn(QS)_2$ complex as well as the protonated form of the sulphonic acid group leading to an increase in the luminescence intensity at 483 nm and thus restoring the original luminescence intensity ratio ($I_{600}/I_{483}$) of WLE QDC. On the other hand, recovering the quenched emission intensity of the dopant emission of $Mn^{2+}$ doped ZnS QD (which occurred during QDC formation) at higher pH – followed by inhibiting the quenching effect of the $Zn(QS)_2$ complex, being attached to the surface of the $Mn^{2+}$ doped ZnS QD (present in WLE QDC) – may be the other reason for the observed changes. This clearly indicates the mutual effect of $Mn^{2+}$ doped ZnS QDs and surface $Zn(QS)_2$ complex, present in WLE QDC, may make them an excellent ratiometric two target-responsive pH nanoprobe in the range of 6.5–10.3.

As is clear from the above results the capability of increasing one emission signal accompanied by a decrease in another emission signal of WLE QDC based on varying the pH of their dispersion, results in a two-target responsive reversible ratiometric nanoprobe, with the advantage of being nontoxic (avoiding the use of heavy metal), color and chromaticity based detection, in comparison to other optical pH nanoprobes (which usually suffer from the drawbacks of toxicity, complicated and costly fabrication strategy, and non-radiative energy transfers). The details of which are summarized in Table S5 (ESI†) and thus indicate their future application potential as ratiometric pH nanoprobes.

In conclusion, the use of nontoxic single component WLE QDC nanoprobe, comprising greenish blue emitting zinc quinolate complex ($\lambda_{em}$ – 483 nm) and orange-red emitting $Mn^{2+}$ doped ZnS QD ($\lambda_{em}$ – 600 nm), as a ratiometric two target based optical sensor of pH, in the physiological range of pH (6.5–10.3), has been demonstrated. Importantly, changes in the luminescence intensity ratio ($I_{600}/I_{483}$), color and chromaticity, based on changes in the pH of the aqueous dispersion of the WLE QDC clearly illustrates their applicability towards pH sensing. Additionally, the reversibility (up to four cycles) in the luminescence intensity $I_{600}/I_{483}$ ratio, based on changing the pH of the WLE QDC indicated their reliability as well as future potential applications.

SB thanks the Department of Science & Technology (DST/INSPIRE/04/2017/001910; IFA17-CH287) Government of India for funding. Assistance from CIF, IIT Guwahati, Uday Pan, Mihir Manna and Milan Mahadani are acknowledged. This paper is dedicated to Prof. Arun Chattopadhyay for his constant support, help and advice.

## Conflicts of interest

There are no conflicts to declare.

## Notes and references

1 X. Huang, J. Song, B. C. Yung, X. Huang, Y. Xiong and X. Chen, *Chem. Soc. Rev.*, 2018, **47**, 2873–2920.
2 S. Silvi and A. Credi, *Chem. Soc. Rev.*, 2015, **44**, 4275–4289.
3 T. Jin, A. Sasaki, M. Kinjo and J. Miyazaki, *Chem. Commun.*, 2010, **46**, 2408–2410.
4 Y. Chen, P. Chen, C. Wang, Y. Lin, C. Ou, L. Ho and H. Chang, *Chem. Commun.*, 2014, **50**, 8571–8574.
5 K. Paek, S. Chung, C. Cho and B. J. Kim, *Chem. Commun.*, 2011, **47**, 10272–10274.
6 R. C. Somers, R. M. Lanning, P. T. Snee, A. B. Greytak, R. K. Jain, M. G. Bawendi and D. G. Nocera, *Chem. Sci.*, 2012, **3**, 2980–2985.
7 I. L. Medintz, M. H. Stewart, S. A. Trammell, K. Susumu, J. B. Delehanty, B. C. Mei, J. S. Melinger, J. B. Blanco-Canosa, P. E. Dawson and H. Mattoussi, *Nat. Mater.*, 2010, **9**, 676–684.
8 P. T. Snee, R. C. Somers, G. Nair, J. P. Zimmer, M. G. Bawendi and D. G. Nocera, *J. Am. Chem. Soc.*, 2006, **128**, 13320–13321.
9 K. Ahmad, S. K. Gogoi, R. Begum, M. P. Sk, A. Paul and A. Chattopadhyay, *ChemPhysChem*, 2017, **18**, 610–616.
10 F. W. Pratiwi, Y. K. Hsia, C. W. Kuo, S. M. Yang, Y. K. Hwu and P. Chen, *Biosens. Bioelectron.*, 2016, **84**, 133–140.
11 S. Bhandari, S. Roy, S. Pramanik and A. Chattopadhyay, *Langmuir*, 2015, **31**, 551.
12 S. Pramanik, S. Bhandari, S. Roy and A. Chattopadhyay, *J. Phys. Chem. Lett.*, 2015, **6**, 1270.
13 B. B. Srivastava, S. Jana, N. S. Karan, S. Paria, N. R. Jana, D. D. Sarma and N. Pradhan, *J. Phys. Chem. Lett.*, 2010, **1**, 1454.
14 R. N. Bhargava, D. Gallagher, X. Hong and A. Nurmikko, *Phys. Rev. Lett.*, 1994, **72**, 416.
15 H. Pan, F. Liang, C. Mao, J. Zhu and H. Chen, *J. Phys. Chem. B*, 2007, **111**, 5767.
16 S. Sapochak, F. E. Benincasa, R. S. Schofield, J. L. Baker, K. K. C. Riccio, D. Fogarty, H. Kohlmann, K. F. Ferris and P. E. Burrows, *J. Am. Chem. Soc.*, 2002, **124**, 6119.
17 T. A. Hopkins, K. Meerholz, S. Shaheen, M. L. Anderson, A. Schimdt, B. Kippelen, A. B. Padias, H. K. Hall, N. Peyghambarian and N. R. Amstrong, *Chem. Mater.*, 1996, **19**, 344.
18 A. Hakonen and J. E. Beves, *ACS Sens.*, 2018, **3**, 2061–2065.
19 A. Hakonen, J. E. Bevesb and N. Stromberg, *Analyst*, 2014, **139**, 3524.
20 A. Hakonen and S. Hulth, *Anal. Chim. Acta*, 2008, **606**, 63.
21 S. Bhandari, S. Roy and A. Chattopadhyay, *RSC Adv.*, 2014, **4**, 24217.
22 D. Zherebetskyy, M. Scheele, Y. Zhang, N. Bronstein, C. Thompson, D. Britt, M. Salmeron, P. Alivisatos and L. Wang, *Science*, 2014, **344**, 1380.
23 D. Jiang, L. Cao, G. Su, H. Qu and D. Sun, *Appl. Surf. Sci.*, 2007, **253**, 9320.
24 M. Banski, M. Chrzanowski, G. Zatryb, J. Misiewicz and A. Podhorodecki, *RSC Adv.*, 2018, **8**, 25417.
25 A. A. Bol and A. Meijerink, *J. Phys. Chem. B*, 2001, **105**, 10203.
26 K. Soroka, R. S. Vithanage, D. A. Phillips, B. Walker and P. K. Dasgupta, *Anal. Chem.*, 1987, **59**, 629.

 